Distinct catecholaminergic pathways projecting to hippocampal CA1 transmit contrasting signals during behavior and learning

Chad M Heer[1], Mark E J Sheffield[1*]

[1]*The Department of Neurobiology, The University of Chicago, Chicago, IL, USA*

Abstract

Neuromodulatory inputs to the hippocampus play pivotal roles in modulating synaptic plasticity, shaping neuronal activity, and influencing learning and memory. Recently it has been shown that the main sources of catecholamines to the hippocampus, ventral tegmental area (VTA) and locus coeruleus (LC), may have overlapping release of neurotransmitters and effects on the hippocampus. Therefore, to dissect the impacts of both VTA and LC circuits on hippocampal function, a thorough examination of how these pathways might differentially operate during behavior and learning is necessary. We therefore utilized 2-photon microscopy to functionally image the activity of VTA and LC axons within the CA1 region of the dorsal hippocampus in head-fixed male mice navigating linear paths within virtual reality (VR) environments. We found that within familiar environments some VTA axons and the vast majority of LC axons showed a correlation with the animals' running speed. However, as mice approached previously learned rewarded locations, a large majority of VTA axons exhibited a gradual ramping-up of activity, peaking at the reward location. In contrast, LC axons displayed a pre-movement signal predictive of the animal's transition from immobility to movement. Interestingly, a marked divergence emerged following a switch from the familiar to novel VR environments. Many LC axons showed large increases in activity that remained elevated for over a minute, while the previously observed VTA axon ramping-to-reward dynamics disappeared during the same period. In conclusion, these findings highlight distinct roles of VTA and LC catecholaminergic inputs in the dorsal CA1 hippocampal region. These inputs encode unique information, likely contributing to differential modulation of hippocampal activity during behavior and learning.

1. Introduction

Catecholamines have a well established role in hippocampal function. Both dopamine and norepinephrine have been shown to impact hippocampal dependent learning and memory [1, 2, 3, 4, 5, 6, 7], alter synaptic plasticity [8, 4, 9, 10, 11, 12], modulate cell excitability [13, 14], and influence the formation and stability of place cells[15, 2], hippocampal neurons that selectively fire at specific locations in an environment [16]. Traditionally, the main source of dopamine to the dorsal hippocampus was thought to be sparse inputs from the ventral tegmental area (VTA), while locus coerulues (LC) inputs provided the main source of norepinphrine.

VTA DA inputs to dorsal CA1 of the hippocampus mainly innervate stratum oriens [17, 18, 19], and their activity bidirectionally modulates Schaffer Collateral (CA3-CA1) synapses [20], enhances persistence of reward-location associations [21], and drives place preference [22]. VTA-hippocampus input activity can also bias place field location [22], improve place field stability across days [21], and drive reward expectation dependent enhancement of place field quality [23]. However, many of the effects of DA modulation of the hippocampus have now been attributed to LC inputs as their activity enhances the strength of Schaffer Collateral synapses [17], improves memory retention [24], improves place field stability across days [25], and can bias place fields to a location when paired with a reward [26] through DA mechanisms. Although many of the effects of LC and VTA are overlapping, potentially indicating shared mechanisms of action, they are believed to play different roles in spatial learning and memory [27]. LC inputs influence the encoding of novel environments [24, 25], while VTA DA inputs increase persistence of reward context associations [21], alter hippocampal neurons firing rate [18], and can bias place preference [22]. It is possible that these differences arise because of the differences in activity observed between LC and VTA DA neurons. Therefore, characterizing the encoding properties of LC and VTA inputs directly in the hippocampus during navigation and spatial learning would provide important insights into the specific roles of these distinct neuromodulatory pathways.

Additionally, recent findings indicate considerable heterogeneity in the activity of VTA [28] and LC [29, 30, 31] neurons, highlighting the need for projection specific recordings. Therefore, we functionally imaged VTA DA and LC axons with single axon resolution in dCA1 of mice as they navigated familiar and novel virtual reality (VR)

*Corresponding author
Email address: sheffield@uchicago.edu (Mark E J Sheffield)

environments for rewards. We observed distinct encoding properties between these sets of inputs during navigation and in response to environmental novelty. During the approach to a previously rewarded location, the activity of most VTA DA axons ramped up. In contrast, most LC axons did not show this ramping activity and instead predicted the start of motion. Additionally, a majority of LC axons and some VTA axons showed activity associated with the animal's velocity. Following exposure to a novel environment, VTA axon ramping-to-reward signals greatly reduced but LC axon activity sharply increased. These findings support distinct roles for VTA and LC inputs to the hippocampus in spatial navigation of rewarded and novel environments.

2. Results

To record the activity of dopaminergic inputs to the dorsal hippocampus, we expressed axon-GCaMP6s or axon-GCaMP7b in LC or VTA neurons of different mice. We utilized the NET-cre mouse line [25] to restrict expression to noradrenergic LC neurons, and the DAT-Cre line [32] to restrict expression to dopaminergic VTA neurons (Fig 1B). Mice were then head-fixed and trained to run a linear virtual reality (VR) track for water rewards delivered at the end of the track (Fig 1A). Following reward delivery, mice were teleported to the beginning of the track and allowed to complete another lap. On experiment day mice navigated the familiar, rewarded VR environment for 10 min while 2-photon microscopy was used to image the calcium activity of LC (87 axons from 22 imaging sites in 16 mice) or VTA (7 axons from 7 imaging sites in 7 mice) axons in the dorsal CA1 (Fig 1C). Based on the z-axis depth of the recording planes, and the presence of increased autofluorescence in stratum pyramidal, we determined all 7 VTA axons were in *Stratum Oriens*, while for LC recordings, 18 sessions (78 axons in 11 mice) occurred in *Stratum Oriens* and 5 sessions (9 axons in 5 mice) in *Stratum Pyramidalis*. Example VTA (left, orange) and LC (right, blue) axon calcium activity aligned to the animal's behavior are shown in Fig 1D. Axons from both brain regions showed periodic activity linked to the animals' exploration of the VR environment.

2.1. Distinct activity dynamics in VTA and LC inputs during rewarded navigation of a familiar environment

To examine axon activity further, we first looked at the mean activity across all axons as a function of track position (Fig 1E). As previously reported [23], VTA DA axons increase activity along the track, peaking at the reward location at the end of the track. In contrast, LC input activity remains relatively constant across all positions along the track (Fig 1Eii). To examine if this difference could be due to the lower sample size of VTA axons compared to LC axons, the LC axons were down-sampled to match the VTA sample size (n = 7) and the slope and intercepts of the down-sampled data was found. This was repeated 1000 times and did not generate any LC data points that overlap with VTA data demonstrating the difference in relationship between position and activity was not due to the different sample sizes (Fig 1Eiii). We also examined the position related activity of individual VTA and LC axons and observed a positive relationship between position and activity in 85.7% of VTA axons (6/7) but only 28.7% of LC axons (25/87) while 42.5% of LC axons (37/87) had a negative relationship between position and activity (Fig 1E.iv.). For a subset of VTA (n = 6) and LC axons (n = 26), the reward at the end of the track was removed, and the activity of these axons in the unrewarded condition was examined (Fig 2A.) While the slope of the VTA population activity across positions significantly decreased (Fig 2B.i.) as expected and previously reported [23], the LC population activity across positions did not significantly change (Fig 2C.i.). This confirmed that the ramping activity in VTA axons was due to the animal's proximity to an expected reward and this signal was not present in the average activity of LC axons.

Next, we investigated the mean activity of these axons as a function of velocity. The population mean of both VTA and LC axons increased as velocity increased (Fig 1F). This is consistent with the finding that LC inputs to dCA1 encode velocity [26] and the finding that DA VTA neurons encode kinematics [28]. Again, to account for differences in sample size, we down sampled the LC axons 1000 times and found the slope and y-intercept of each sampling. The overlap of the VTA and LC slopes and intercepts confirms we cannot conclude any differences in velocity related activity in the VTA and LC axon populations (Fig 1F.iii.). However, we observed a statistically significant positive relationship between velocity and activity in the majority, 72.4%, of LC axons (63/87), while only 28.6% (2/7) of VTA axons showed a positive relationship with velocity. (Fig 1F.iv). The strong velocity correlated activity in a small subset of VTA DA axons indicates heterogeneity in the activity of these inputs similar to what is observed in VTA DA cell bodies [28]. To determine if the velocity correlated activity in VTA DA axons is confounded by the ramping to reward activity, we examined this activity in the unrewarded condition where the ramping to reward activity is absent. Here, the VTA population activity across all velocities is decreased but the slope, or the relationship between velocity and activity, remains unchanged (Fig 2B.ii.). This is consistent with a subset of VTA axons encoding velocity information, while the overall decrease in activity is explained by the decrease in reward related activity demonstrated in Fig 2B.i. On the other hand, the relationship between velocity and LC activity is unchanged in the unrewarded environment(2C,ii), indicating condition invariant velocity encoding in LC axons.

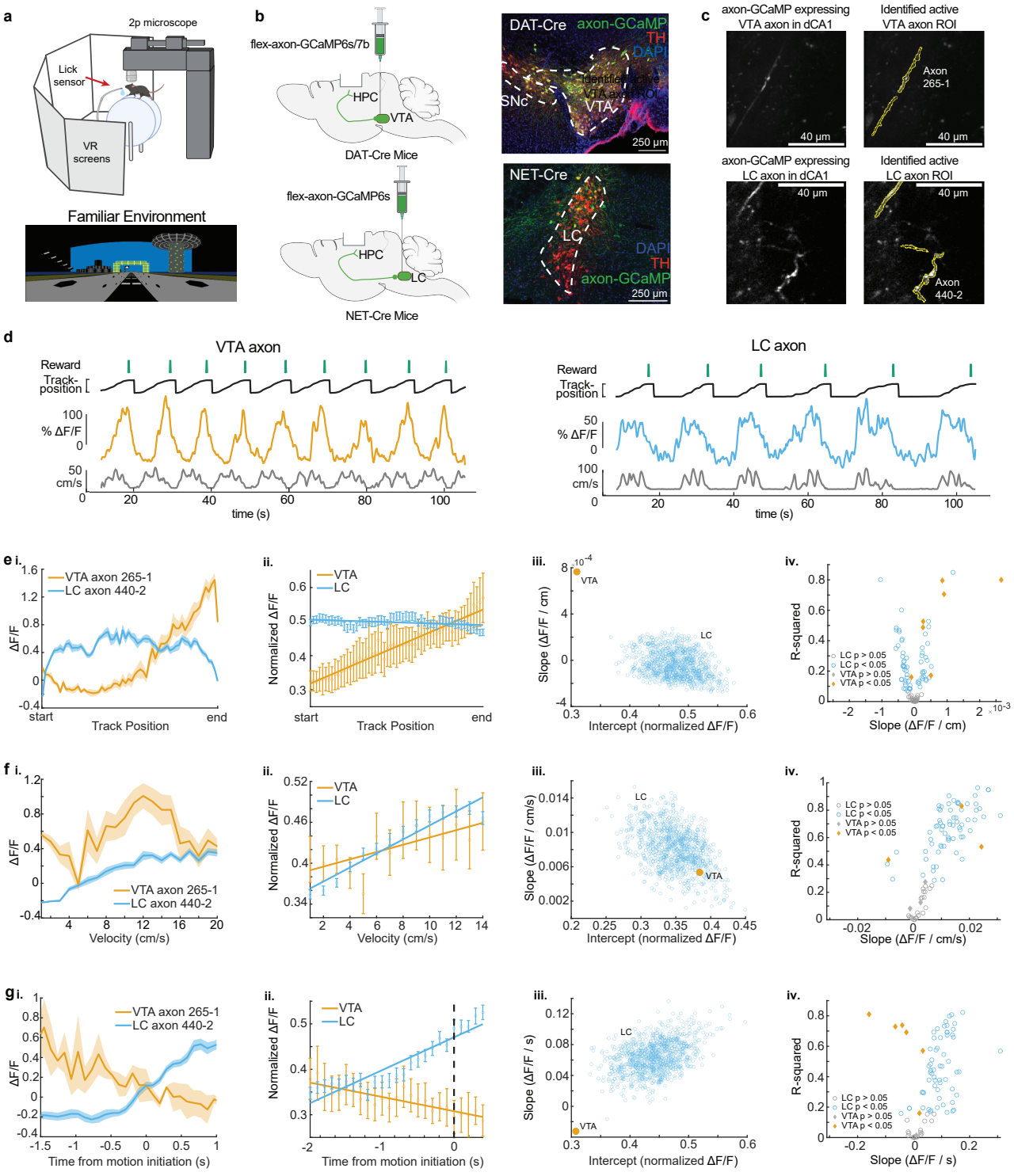

Figure 1. Distinct activity dynamics in VTA and LC axons during navigation of familiar environments a, Experimental setup (top), created with BioRender.com. Example virtual reality environment. **b,** Schematic representation of injection procedure (left). Representative coronal brain sections immunostained for Tyrosine Hydroxolase (TH) from a DAT-Cre mouse showing overlapping expression of axon-GCaMP (green) and TH (red) in VTA neurons (top) and from a NET-Cre mouse showing overlapping expression of axon-GCaMP(green and TH (red) in LC neurons (bottom). **c,**. Example CA1 field of view of VTA axons (top) and LC axons (bottom). Extracted regions of interest used for example VTA and LC activity throughout the figure. **d,** Example DAT-Cre mouse (left) and NET-Cre mouse (right) with aligned reward delivery (top, green), mouse track position (black), $\Delta F/F$ from example roi (VTA-orange, LC-blue), and mouse velocity (bottom, gray).

Finally, we examined the activity of LC and VTA axons during rest and the transition to movement. The population of LC axons ramped up in activity during the 2 s leading up to motion onset (Fig 1G). This is consistent with reports of activity of LC axons in cortical areas [33] showing LC activity prior to motion onset. In contrast, VTA axons show decreasing activity during the 2 s leading up to motion onset (Fig 1G). This ramping down in VTA axon activity is likely due to most periods of immobility occurring between reward delivery and the start of the next lap, during which we previously demonstrated reward related activity ramps down in VTA axons [23]. Indeed, in the unrewarded condition the negative slope of the VTA population activity leading up to motion onset disappears (Fig 2B.iii.), indicating this relationship is largely driven by the presence of reward rather than motion onset. However, the LC population activity remains unchanged in the unrewarded environment (Fig 2C.iii.), suggesting this activity is related to the lead up to motion initiation. These differences in activity are not an artifact of lower sample size of VTA axons as shown by down-sampling the LC axon activity 1000 times and measuring the slopes and intercepts of the down-sampled data did not generate any data points that overlapped with the VTA slope and intercept (Fig 1G.iii). In further support of distinct activity profiles leading up to motion onset, we found that the majority (4/7) of VTA axons decreased in activity leading up to motion onset but only 2/87 LC axons decreased in activity, while the majority, (56/87), of LC axons increased in activity leading up to motion onset (Fig 1G.iv). Together, this analysis demonstrates overlapping but distinct activity in VTA and LC axons during spatial navigation with VTA axons showing strong activity correlated with distance to reward and some velocity correlated activity, while LC axons demonstrate activity correlated to velocity and time to motion onset.

2.2. Environmental Novelty induces activity in LC but not VTA inputs

Both LC and VTA neurons have been shown to respond to novel environments [17]. Therefore, we aimed to examine the activity of VTA DA and LC inputs to the hippocampus during exposure to novel VR environments. Following 10 minutes in the familiar environment, mice were teleported to a novel VR environment of the same track length, with a reward at the same position at the end of the track. Following teleportation, we found the running speed of mice transiently decreases (Fig 3A) and they spend less time immobile (Fig 3A), demonstrating mice recognize they are navigating a novel environment.

We aligned VTA and LC axon activity to the switch to the novel environment and investigated changes in activity due to exposure to novelty. To test whether the mean axon activity is significantly elevated or lowered, we defined a baseline by generating 1000 shuffles of the axon traces across the entire recording sessions, downsampling the shuffled data 1000 times to match the VTA (n = 7) and LC (n = 87) sample sizes, and calculating the mean and 95% CI of the shuffled data. After teleportation, the periodic activity observed in the mean of VTA axons, likely reflecting ramping-to-reward signals in each individual axon, dramatically disappears (Fig 3B). This is evident in the traces of most of the individual VTA axons showing a loss of the ramping-to-reward signal (Fig 3C), and in the VTA population position binned activity showing a significant reduction in ramping activity (Fig 1).

Strikingly, LC axons show a dramatic increase in mean activity that remains elevated for ¿ 1 minute following exposure to the novel environment (Fig 3B) similar with findings that LC cell body activity is elevated for minutes following exposure to environmental novelty [17]. A significant increase in activity above baseline activity following the switch to a novel environment can be seen in 36 LC neurons (Fig 3C). To further characterize this activity, we found the mean population activity for each lap and separately for 10 s time bins leading up to and following exposure to the novel environment. This analysis shows that LC activity is significantly elevated above baseline for 6 consecutive laps and approximately 90 seconds following exposure to the novel environment (Fig 3D). These findings demonstrate that LC inputs signal environmental novelty, supporting a role for these inputs in novelty encoding in the hippocampus.

2.3. Novelty-induced changes in behavior explains the late but not early increases in LC activity

It is possible that the change in the amount of time the animals spend running versus immobile in the novel environment could explain the increase in LC activity in the novel environment, as LC activity is related to behavior (Fig. 1). For instance, LC axons show elevated activity during motion versus rest (Fig. 1G) . Therefore, an increase in the time spent in motion upon exposure to the novel environment could lead to an increase in LC activity. To account for the differences in time spent running vs immobile between the two environments, we removed any periods where the mice were immobile to isolate the effects of novelty from changes in behavior (Fig 3A). When only looking at activity during running in both environments, we found that LC axon activity is elevated for 2 laps, or 40 s, in the novel environment (Fig 4B-E). This indicates that there are two separate components that drive LC axon activity during the initial exposure to the novel environment. One, a shorter purely novelty-induced increase in activity which occurs during the first 2 laps, or about 40 s, in the novel environment. Two, a behavior-induced increase in LC activity caused by an increase in the percentage of time spent running that extends beyond the increase in the novelty-induced activity for 6 laps or 90 s.

If the short, novelty-induced signal in LC axons is an additional signal riding on top of the behavior correlated signals - position, velocity, and motion onset- we would

Figure 1 *(continued)*: **e, i,** Position binned $\Delta F/F\pm$ s.e.m in example VTA (orange) and LC (blue) ROIs during navigation of the familiar rewarded environment. **ii,** Population average position binned $\Delta F/F\pm$ s.e.m. in VTA ROIs (orange, n = 7 ROIs in 7 mice) and LC ROIs (blue, n = 87 ROIs from 27 sessions in 17 mice) . Linear regression analysis (on all data points, not means) shows that the population of VTA ROIs increase activity during approach of the end of the track while the population of LC ROIs have consistent activity throughout all positions. Linear regression, F test, VTA, $P < 1e-21$, LC, $P < 0.01$. **iii,** The LC data set was resampled 1000x using n = 7 axons to match the number of VTA Rois and the slope and intercept of the regression line were measured each time (blue dots). The VTA slope is steeper than all LC slopes indicating a stronger positive relationship between position and activity for VTA inputs. **iv**, Linear regression of position binned activity of individual VTA (orange diamonds), and LC (blue, circles) axons. The majority (6/7) of VTA axons show a significant positive relationship with position while LC axons show both a positive (25/87) and negative (37/87) relationship. **F, i,** Same example ROIs as (d) binned by velocity. **ii,** Same data as (d, ii,) binned by velocity. Linear regression shows that the population of VTA and LC ROIs have a significant relationship with velocity. Linear regression, F test, VTA, $P < 0.05$, LC,$P < 1e-68$. **iii,** Resampling shows the VTA slope and intercept is within the resampled LC slopes and intercepts indicating similar relationships with velocity. **iv,** Linear regression of individual VTA and LC axons shows the majority (63/87) of LC axons have a significant positive relationship with velocity while only 2 VTA axons show this relationship. **g,** Same example ROIs as (d) aligned to motion onset. **ii,** Same data as (d, ii,) aligned to motion onset. Linear regression shows that the population of VTA axons have a negative slope prior to motion onset while LC axons have positive slope. Linear regression, F test, VTA, $P < 0.01$, LC, $P < 1e-65$. **iii,** Resampling shows the VTA slope is negative while all resampled LC slopes are positive. **iv,** Linear regression of individual VTA and LC axons shows the majority (56/87) of LC axons have a significant positive slope prior to motion onset while the majority (4/7) of VTA axons have a negative slope.

expect a disruption of these behavioral correlations during the initial lap in a novel environment. To test this we examined these behavioral correlations lap-by-lap following exposure to the novel environment. Indeed, the slopes of the position binned, velocity binned, and motion onset aligned data are all significantly more negative in the first lap in the novel environment than the final laps of the familiar environment (Fig 4F-H). This is consistent with a decaying novelty signal that peaks at the start of the first lap and rides on top of these behaviorally-correlated signals. This produces an elevation in activity at positions near the start of the first lap that is lower at positions near the end of the first lap, causing a negative slope relationship between position and LC axon activity on the first lap (Fig. 4F; light green line). Further, low velocities occur at the start of each lap compared to the end of the lap. Because the novelty signal is highest when animals are running slowest, the novelty signal flattens the velocity-LC activity relationship (Fig. 4G; light green line). Lastly, rest periods typically occur at the start of the track. Therefore, motion onset encoding on the first lap in the novel environment occurs when the novelty signal is highest, again, flattening the relationship (Fig. 4H; light green line). By the third lap in the novel environment, where the novelty-induced signal is no longer observable, the relationships between LC activity and position is no longer different than the relationship in the familiar environment (Fig 4F, -green). The relationship between LC activity and motion onset is also no longer different by the third lap in the novel environment (Fig 4H). Although the relationship between velocity and LC activity is different in the third novel lap than that of the final familiar laps, by the final lap in the novel environment it is no longer different than the familiar relationship(Fig 4G). Together this demonstrates that the relationships between LC activity and behavior in the novel environment quickly return to those in the familiar environment. Interestingly, the slope is significantly increased in the final lap of the novel environment (Fig 4F), potentially indicating the development of activity at the novel reward location as has been previously reported [26]. Altogether, examining the lap-by-lap dynamics of the position, velocity, and motion onset activity indicates that environmental novelty induces a sharp increase in LC input activity during the first two laps in the novel environment while also inducing a change in behavior that leads to increased LC input activity in subsequent laps.

3. Discussion

During spatial navigation in a familiar environment, activity of VTA DA inputs to dCA1 were strongly modulated by position relative to reward, ramping up as mice approached the end of the track where reward was located. We have previously shown that this activity is dependent on the history of reward delivery and reflects the animals' reward expectation [23]. VTA axons in dCA1 also showed decreasing activity during rest prior to motion onset. However, after removing reward, VTA axons showed no activity prior to motion onset indicating this relationship was driven by reward related activity.

On average, VTA axons showed activity modulated by velocity in a familiar rewarded environment. This relationship was largely due to the activity of two VTA axons that were strongly modulated by velocity, suggesting that there is heterogeneity in the population of VTA axons in dCA1. A positive relationship between average VTA axon activity and velocity persisted in the unrewarded condition and in the novel environment, indicating velocity encoding in these inputs that is not a result of reward related activity. This heterogeneity in the encoding across individual VTA axons is consistent with studies demonstrating heterogeneous encoding of behavioral variables in VTA DA cell bodies, including activity related to rewards and kinematics [28].

Our findings that VTA DA axons show no novelty induced activity and instead show reduced activity following exposure to a novel environment, is in contrast with several studies showing novelty induced activity in VTA DA

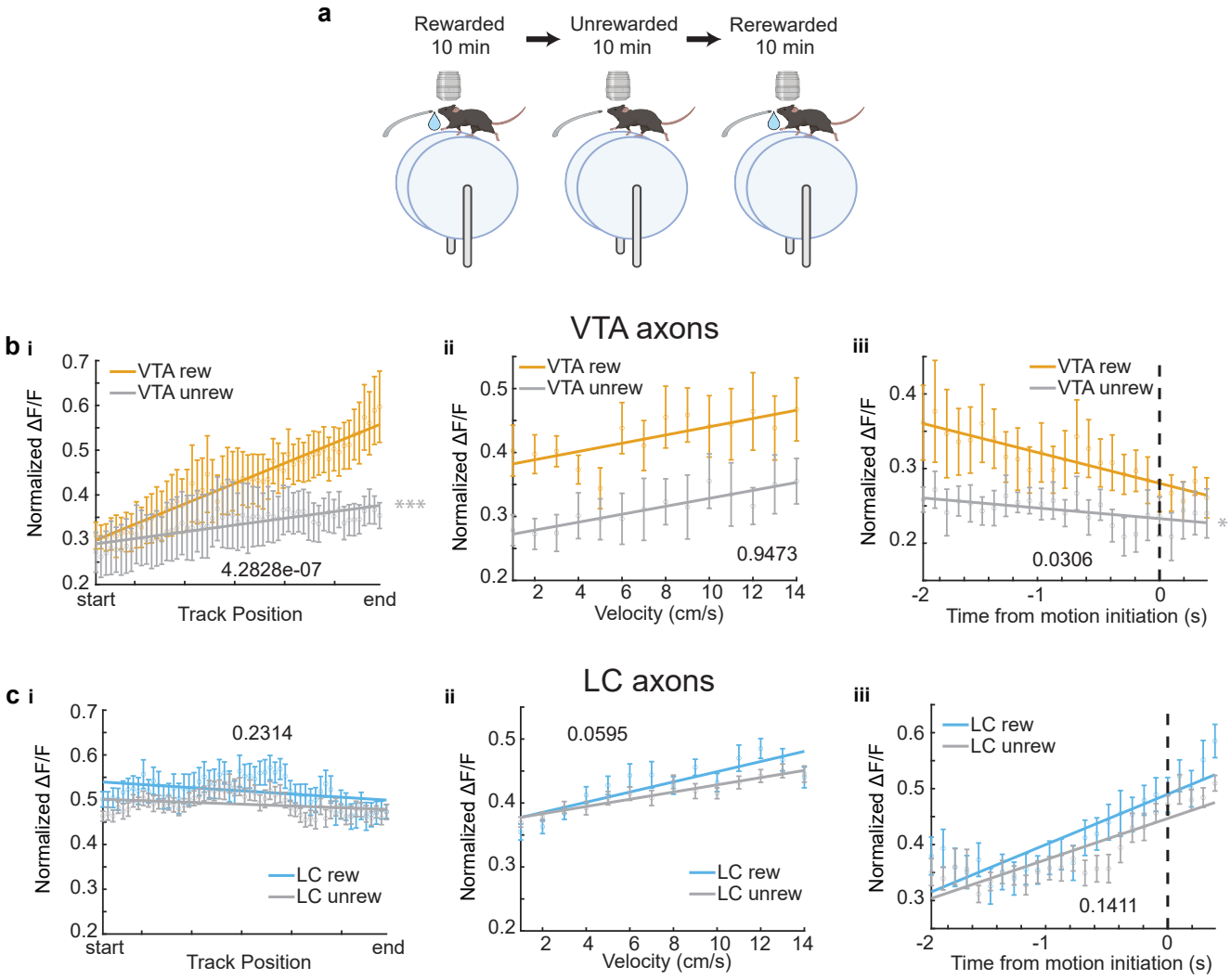

Figure 2: **Removal of reward restructures VTA but not LC input activity during spatial navigation: a.** Experimental Paradigm. **b.i.** Population average position binned $\Delta F/F \pm$ s.e.m. of VTA ROIs (n = 6 ROIs in 6 mice) in the rewarded (VTA rew, orange) and unrewarded conditions (VTA unrew, gray). Linear regression, F test, Rewarded, $P < 1e-22$, Unrewarded, $P < 0.001$. **ii**. Same data as (b,i) binned by velocity. Linear regression, F test, Rewarded, $P < 0.05$, Unrewarded, $P < 0.05$. **iii**, Same data as (b,i) aligned to motion onset. Linear regression, F test, Rewarded, $P < 1e-4$, Unrewarded, $P < 0.05$. **c, i,** Population average position binned $\Delta F/F \pm$ s.e.m. of LC ROIs (n = 26 ROIs in 7 sessions in 4 mice) in the rewarded (LC rew, blue) and unrewarded conditions (LC unrew, gray). Linear regression, F test, Rewarded, $P < 0.01$, Unrewarded, $P < 0.01$. **ii,** Same data as (c,i) binned by velocity. Linear regression, F test, Rewarded, $P < 1e-12$, Unrewarded, $P < 1e-15$. **iii,** Same data as (c,i) aligned to motion onset. Linear regression, F test, Rewarded, $P < 1e-21$, Unrewarded, $P < 1e-26$. The slope of each unrewarded measure was compared to the familiar laps using a one-way ANCOVA with Tukey HSD post hoc test. * $P < 0.05$, ** $P < 0.001$, *** $P < 1e-4$.

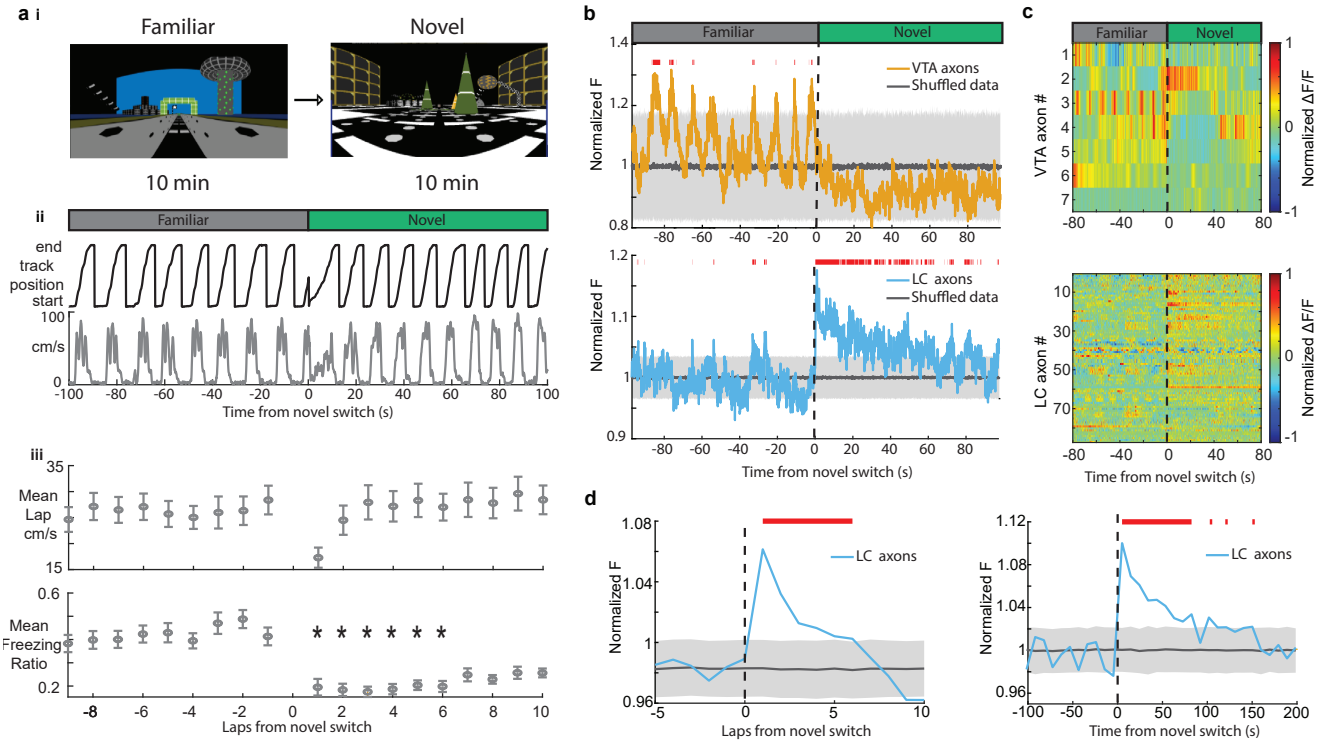

Figure 3: **Exposure to a novel environment causes an abrupt and sustained increase in activity in LC but not VTA inputs to dCA1 a, i,** Experimental Paradigm. **ii,** Behavior from example mouse during the transition from the familiar VR environment to a novel VR environment showing the animals track position (top, black) and velocity (bottom, gray). **iii,** The average running velocity ± s.e.m. of all mice during the transition to a novel VR environment (top). The average freezing ratio of all mice ± s.e.m., calculated as the time spent immobile (velocity < 5cm/s) divided by the total lap time. Each lap was compared to the first lap in F using a one-way ANOVA with Tukey HSD post hoc test. * $P < 0.05$ **b,** Mean normalized F of all VTA ROIs (top, n = 7) and LC ROIs (bottom, n = 87) aligned to the switch to the novel environment. To define a baseline and 95% CI (gray shaded region), 1000 shuffles were created from the calcium traces and down sampled to match the sample size and averaged. This was repeated 1000 times and the mean and 95% CI of this shuffled data was determined for each frame. Red lines indicate periods where two or more consecutive frames passed above the % CI of the shuffled baseline. **c,** Normalized $\Delta F/F$ activity of all VTA ROIs (top) and LC ROIs (bottom) aligned to the switch to the novel VR environment. **d,** The normalized fluorescence of all LC ROIs binned by lap (left) or into 50 frame bins (right). The baseline and 95% CI (gray shaded region) was defined using the same method as in (b) Red lines indicate bins above the baseline 95% CI.

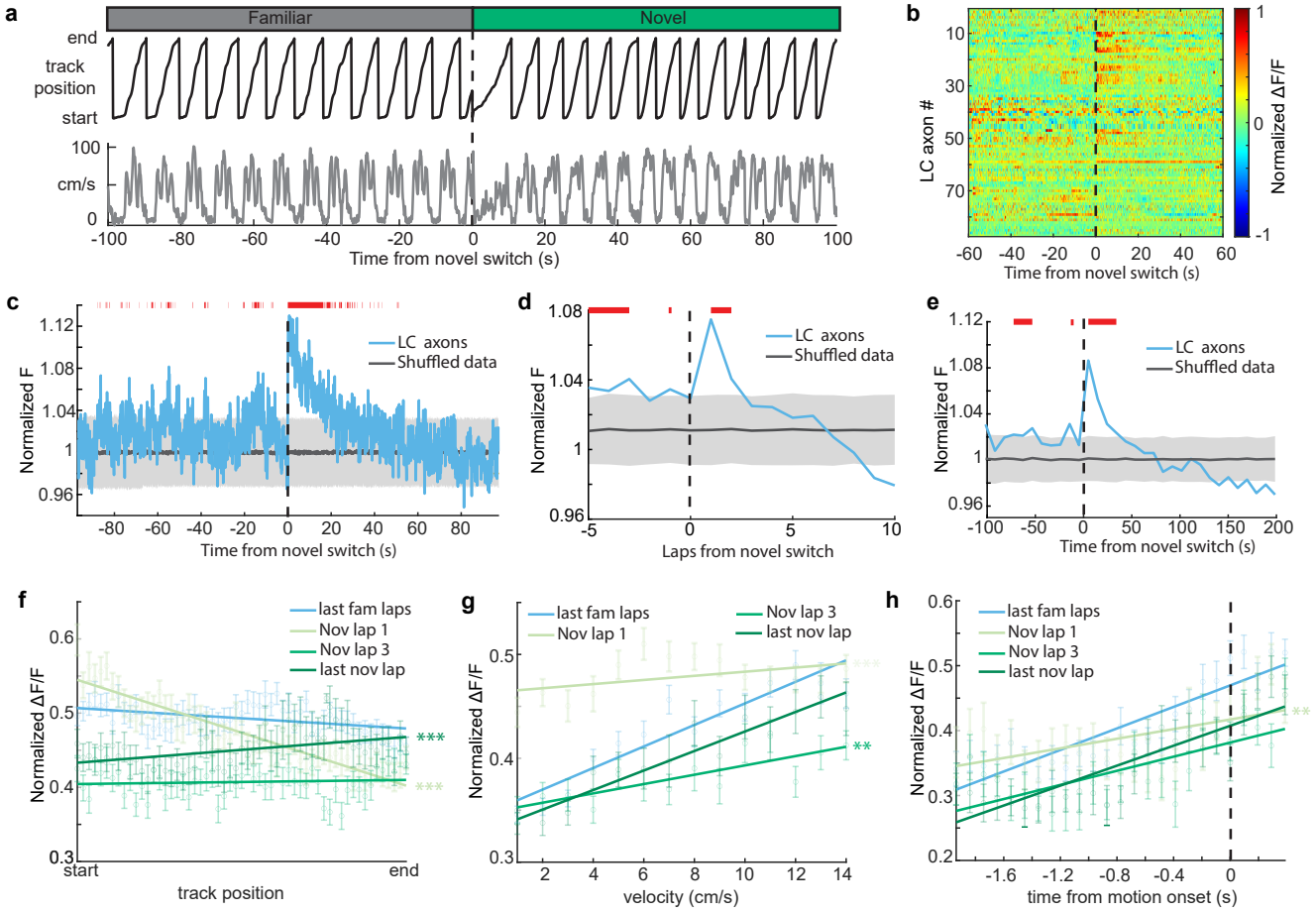

Figure 4: **Novelty-induced changes in behavior explain the late but not early increases in LC activity a,** Good behavior from example mouse following removal of freezing periods (velocity < 0.2 cm/s) during the transition from the familiar to a novel VR environment showing the animals track position (top, black) and velocity (bottom, gray). **b,** Normalized $\Delta F/F$ activity of all LC ROIs aligned to the switch to the novel VR environment following removal of freezing periods. **c,** Mean normalized F of all VTA ROIs (top, n = 7) and LC ROIs (bottom, n = 90) aligned to the switch to the novel environment. To define a baseline and 95% CI (gray shaded region), 1000 shuffles were created from the calcium traces and down sampled to match the sample size and averaged. This was repeated 1000 times and the mean and 95% CI of this shuffled data was determined for each frame. Red lines indicate periods where two or more consecutive frames passed above the 95% CI of the shuffled baseline. **d,e,**. The normalized F of all LC ROIs binned by lap (d) or into 50 frame bins (e). The baseline and 95% CI (gray shaded region) was defined using the same method as in (c). Red lines indicate bins above the baseline 95% CI. **f-h,** Population average position binned (f), velocity binned (g), and motion onset aligned (h) $\Delta F/F \pm$ s.e.m. in LC ROIs (n = 90) in the final laps of the familiar environment (light blue), and the first (orange), third (dark blue), and final laps (green) of the novel environment. Linear regression, F test, position binned (f) fam last, $P < 1e-4$, nov 1, $P < 1e-68$, nov 3, $P = 0.48$, nov last, $P < 0.001$; velocity binned (g) fam last, $P < 1e-31$, nov 1, $P < 0.05$, nov 3, $P < 1e-5$, nov last, $P < 1e-13$; motion onset aligned (h) fam last, $P < 1e-29$, nov 1, $P < 0.001$, nov 3, $P < 1e-9$, nov last, $P < 1e-18$. The slope of each lap was compared to the final familiar laps using a one-way ANCOVA with Tukey HSD post hoc test. * $P < 0.01$, ** $P < 0.001$, *** $P < 1e-4$.

cell bodies [17, 27, 34], indicating potential heterogeneity in VTA neurons in response to novelty. It is possible that some VTA DA inputs to dCA1 respond to novel environments, and the small number of axons recorded here are not representative of the whole population. Another possibility is that the lack of a novelty response we observe is due to differences in experimental design. Here, mice learned to approach a location for reward which has been shown to lead to ramping activity in dopaminergic VTA neurons [35, 23, 36, 37, 38]. Following exposure to novelty, the disappearance of reward related activity could obscure any novelty induced increases in activity. Therefore, additional experiments should be conducted to investigate the heterogeneity of these axons and their activity in different experimental conditions.

LC axons showed no position encoding. Instead, they were modulated by velocity and ramped up in activity prior to motion initiation, consistent with recordings of LC axons by others in dCA1 [26] and in the cortex [33], respectively. An important question is how is this LC axon activity impacting hippocampal neurons during navigation in a familiar environment? It is possible that LC axons during navigation provide increases in excitability that promotes place cell activity as both dopamine and norepinephrine in the hippocampus can impact cell excitability [14, 39, 13]. Additionally, place cells are flexible during spatial navigation with new place fields forming in familiar environments [40, 41] and shifting position with time/experience [41]. Place fields can also shift to follow changing reward [42]and object locations [43]. Dopamine and norepinephrine have also been shown to impact hippocampal synaptic plasticity [44, 39, 11, 12]. Therfore, LC inputs may promote the plasticity necessary for place cells to flexibly adapt to changes in a familiar environment [26, 45]. In other words, LC inputs could allow the hippocampus to be flexible during navigation through their impacts on synaptic plasticity [17, 46, 27].

Exposure to environmental novelty leads to an increase in dopamine in the dorsal hippocampus [47] and promotes synaptic plasticity [48, 11], hippocampal replay [21, 49] and memory persistence [48, 50]. In our experiment, exposure to a novel environment caused an increase in LC axon activity but not in VTA DA axon activity, supporting findings that novel experiences induce activity of LC neurons [17]. The activity of LC neurons in turn increases hippocampal neuron activity [25], increases efficacy of Schaffer Colateral synapses [17], stabilizes place cells across days [25] and memory persistence [25, 17, 51] through dopamine receptor dependent mechanisms. Importantly, while LC inputs to CA1 have been shown to cause an increase in activity [25, 51], shape over-representation of novel reward locations [26], and modulate memory linking [51], they have not been shown to play a role in the formation of contextual memories [51] or stabilization of place cell maps across days [25] in dCA1. However, it is possible this novelty induced activity in LC inputs to dCA1 impacts the formation of instant place fields observed in novel environments [40, 41]. Instant place fields form on the first lap of a novel environment, right when the LC novelty signal is highest in dCA1, suggesting LC inputs may play a role in their formation or stabilization. Therefore, further experiments should investigate the role of LC axons on dCA1 place fields on a trial-by-trial basis.

While LC neurons have been shown to impact novelty encoding through dopaminergic mechanisms [25, 17, 51], this does not exclude the possibility that they also release norepinephrine during exposure to novelty and exploration of a familiar environment. Indeed, hippocampal levels of norepinephrine also increase during exposure to environmental novelty [52, 53], but how this norepinephrine release effects hippocampal function is not well understood. Additionally, it is not known whether norepinephrine and dopamine are released from the same LC inputs or from distinct sets of LC inputs. Dopamine is in the synthesis pathway of norepinephrine and in LC neurons it is loaded into vesicles where it is then converted to norepinephrine by dopamine β-hydroxylase [54]. It is possible that high levels of activity of LC inputs, like those occurring during exposure to novelty, lead to release of vesicles before dopamine can be converted to norepinephrine thus leading to the release of dopamine under these conditions. However, low levels of LC activation, like those observed during familiar environment exploration, may provide time for dopamine to be converted to norepinephrine and thus lead to the release of norepinephrine from LC terminals under these conditions. Further experiments investigating the dynamics of dopamine conversion and release from LC terminals in the hippocampus should be conducted to test this hypothesis.

Here we show that LC input activity is modulated by velocity, time to motion onset, and exposure to novel environments. Each of these conditions is associated with an increase in arousal, and LC activity has been strongly linked to arousal levels []. Therefore, rather than encoding each of these variables independently, LC inputs are likely encoding the animals arousal level during spatial navigation. It has been shown that attention and arousal levels impact tuning properties in many cortical areas and this is thought to be mediated through LC activity[55, 56, 57, 58]. Similarly, changes in the animals' brain state, including changes in attention [15] and engagement [59], alter the tuning properties of place cells. This indicates arousal could impact the function of hippocampal neurons through these LC inputs.

The distinct activity dynamics exhibited by LC and VTA DA axons during spatial navigation of familiar and novel environments underscore their distinct contributions to hippocampal dependent learning and memory processes. Notably, these findings reinforce the notion that VTA DA inputs play a pivotal role in the ongoing maintenance and updating of associations between expected rewards and the locations that lead to them, while LC axons appear to be integral to the process of encoding memories of entirely new environments and stimuli.

4. Methods

4.1. Subjects

All experimental and surgical procedures were in accordance with the University of Chicago Animal Care and Use Committee guidelines. For this study, we used 10–20 week-old male Slc6a3Cre+/- (DAT-Cre+/-) mice and Slc6a2 Cre+/- (NET-Cre+/-)(23–33 g). Male mice were used over female mice due to the size and weight of the head-plates (9.1 mm × 31.7 mm, 2 g) which were difficult to firmly attach on smaller female skulls. Mice were individually housed in a reverse 12 h light/dark cycle at 72 °F and 47% humidity, and behavioral experiments were conducted during the animal's dark cycle.

4.2. Mouse surgery and viral injections

Mice were anesthetized (1–2% isoflurane) and injected with 0.5 ml of saline (intraperitoneal injection) and 0.05 ml of Meloxicam (1–2 mg/kg, subcutaneous injection) before being weighed and mounted onto a stereotaxic surgical station (David Kopf Instruments). A small craniotomy (1–1.5 mm diameter) was made over the ventral tegmental area (VTA) (± 0.5 mm lateral, 3.1mm caudal of Bregma) of DAT-Cre+/- mice or over the locus coeruleus (LC) (± 0.875 mm lateral, -5.45 mm caudal of Bregma). The genetically-encoded calcium indicator, pAAV-hsyn-Flex-Axon-GCaMP6s (pAAV-hSynapsin1-FLEx-axon-GCaMP6s was a gift from Lin Tian (Addgene viral prep # 112010-AAV5 ; http://n2t.net/addgene:112010 ; RRID:Addgene 112010) was injected into the VTA of DAT-Cre+/- mice (200 nL at a depth of 4.4 mm below the surface of the dura) or the LC of NET-Cre+/- mice (200 nL at a depth of 3.65 mm below Bregma). For a subset (4/7) of VTA recordings, a different GCaMP variant, pAAV-Ef1A-Flex-Axon-GCaMP7b, was injected due to the difficulty finding and recording VTA axons in dCA1 (pAAV-Ef1a-Flex-Axon-GCaMP7b (pAAV-Ef1a-Flex-Axon-GCaMP7b was a gift from Rylan Larsen - Addgene plasmid # 135419; http://n2t.net/addgene:135419; RRID: Addgene 135419). Following injections, the site was covered up using dental cement (Metabond, Parkell Corporation) and a metal head-plate (9.1 mm × 31.7 mm, Atlas Tool and Die Works) was also attached to the skull with the cement. Mice were separated into individual cages and water restriction began 3 weeks later (0.8–1.0 ml per day). Mice then underwent surgery to implant a hippocampal window as previously described [60]. Following implantation, the headplate was attached with the addition of a head-ring cemented on top of the head-plate which was used to house the microscope objective and block out ambient light. Post-surgery mice were given 2–3 ml of water/day for 3 days to enhance recovery before returning to the reduced water schedule (0.8–1.0 ml/day).

4.3. Behavior and virtual reality

Our virtual reality (VR) and treadmill setup was designed similar to previously described setups [40, 61]. The virtual environments that the mice navigated through were created using VIRMEn [62]. 2 m (DAT-Cre mice) or 3 m (NET-Cre mice) linear tracks rich in visual cues were created that evoked numerous place fields in mice as they moved along the track at all locations (Fig. 1) [43]. Mice were head restrained with their limbs comfortably resting on a freely rotating styrofoam wheel ('treadmill'). Movement of the wheel caused movement in VR by using a rotatory encoder to detect treadmill rotations and feed this information into our VR computer, as in refs. [40, 61]. Mice received a water reward (4 µL) through a waterspout upon completing each traversal of the track (a lap), which was associated with a clicking sound from the solenoid. Licking was monitored by a capacitive sensor attached to the waterspout. Upon receiving the water reward, a short VR pause of 1.5 s was implemented to allow for water consumption and to help distinguish laps from one another rather than them being continuous. Mice were then virtually teleported back to the beginning of the track and could begin a new traversal. Mouse behavior (running velocity, track position, reward delivery, and licking) was collected using a PicoScope Oscilloscope (PICO4824, Pico Technology, v6.13.2). Behavioral training to navigate the virtual environment began 4–7 days after window implantation (30 min per day) and continued until mice reached ¿2 laps per minute, which took 10–14 days (although some mice never reached this threshold). Mice that reached this behavioral threshold were imaged the following day.

4.4. Two-photon imaging

Imaging was done using a laser scanning two-photon microscope (Neurolabware). Using a 8 kHz resonant scanner, images were collected at a frame rate of 30 Hz with bidirectional scanning through a 16x/0.8 NA/3 mm WD water immersion objective (MRP07220, Nikon). GCaMP6s and GCaMP7b were excited at 920 nm with a femtosecond pulsed two photon laser (Insight DS + Dual, Spectra-Physics) and emitted fluorescence was collected using a GaAsP PMT (H11706, Hamamatsu). The average power of the laser measured at the objective ranged between 50–80 mW. A single imaging field of view (FOV) between 400–700 µm equally in the x/y direction was positioned to collect data from as many VTA or LC axons as possible. Time-series images were collected from 3-5 planes spaced 2 um apart using an electric lens to ensure axons remained in a field of view and reduce power going to an individual plane. Images were collected using Scanbox (v4.1, Neurolabware) and the PicoScope Oscilloscope (PICO4824, Pico Technology, v6.13.2) was used to synchronize frame acquisition timing with behavior.

4.5. Imaging sessions

The familiar environment was the same environment that the animals trained in. The experiment protocol for single day imaging sessions is shown in Fig. 1. Each trial lasted 8–12 min and was always presented in the same

order. Mice were exposed to the familiar rewarded environment for 10 minutes, then were immediately teleported to the start of a novel rewarded VR environment and allowed to navigate for 10 minutes. Mice on average ran 19 ± 3.8 (mean ± 95% CI) laps in the familiar environment, at which point they were teleported to the novel environment and imaging continued for 30 ± 5.4 laps. The Novel-rewarded environment (N) had distinct visual cues, colors and visual textures, but the same dimensions (2 or 3 m linear track) and reward location (end of the track) as the familiar environment. Imaging sessions with large amounts of drift or bleaching were excluded from analysis (8 sessions for NET mice, 6 sessions for LC Mice).

4.6. Histology and brain slices imaging

We checked the expression axon-GCaMP to confirm expression was restricted to the VTA of DAT-Cre mice and the LC of NET-Cre. Mice were deeply anesthetized with isoflurane and perfused with 10 ml phosphate-buffered saline (PBS) followed by 20 mL 4% paraformaldehyde in PBS. The brains were removed and immersed in 30% sucrose solution overnight before being sectioned at 30 µm-thickness on a cryostat. Brain slices were collected into well plates containing PBS. Slices were washed 5 times with PBS for 5 min then were blocked in 1% Bovine Serum Albumin, 10% Normal goat serum, 0.1% Triton X-100 for 2 h. Brain slices were then incubated with 1:500 rabbit-α-TH (MAB318, Sigma Aldrich) and 1:500 mouse-α-GFP (SAB2702197, Sigma Aldrich)in blocking solution at 4 ° C. After 48 h, the slices were incubated with 1:1000 goat-α-rabbit Alexa Fluor 647nm secondary antibody (A32731, ThermoFisher) and 1:1000 goat-α-mouse Alexa Fluor 488nm (A32723, ThermoFisher) for 2 h. Brain slices were then collected on glass slides and mounted with a mounting media with DAPI (SouthernBiotech DAPI-Fluoromount-G Clear Mounting Media, 010020). The whole-brain slices were imaged under ×10 and x40 with a Caliber I.D. RS-G4 Large Format Laser Scanning Confocal microscope from the Integrated Light Microscopy Core at the University of Chicago.

4.7. Image processing and ROI selection

Time-series images were preprocessed using Suite2p (v0.10.1)79. Movement artifacts were removed using rigid and non-rigid transformations and assessed to ensure absence of drifts in the z-direction. Datasets with visible z-drifts were discarded (8 sessions). For axon imaging, ROIs were first defined using Suite2p and manually inspected for accuracy. ROIs were then hand drawn over all segments of Suite2p defined active axons using ImageJ to ensure all axon segments were included for analysis. Fluorescent activity for each ROI was extracted and highly correlated ROIs (Pearson correlation coefficient $\geq$ 0.7) were combined and their fluorescent activity was extracted. To be included Baseline corrected $\Delta F/F$ traces across time were then generated for each ROI using both a small window of 300 frames for lap by lap analysis, and a larger sliding window of 2000 frames to avoid flattening slow signals for novelty response analysis. Additional ROIs were drawn over autofluorescent structures that were not identified by suite2p. These "blebs" were processed in the same way as axon ROIs and used as controls to check for imaging and motion artifacts.

To remove low signal to noise axons, we defined the SNR of each ROI using the power spectrum of their fluorescent activity similar to [33]. For frequencies above 1Hz, the power was defined as noise because this sits outside of the range of frequencies possible for GCaMP6s fluorescence. The SNR ratio was then defined as the ratio of the peak power between 0.5 Hz and 1Hz over the average power between 1 Hz and 3 Hz. The SNR of "blebs" was also determined and any axon with a SNR greater than 1.5 std from the mean of the "blebs" SNR was used for analysis (110/231 LC ROIs, 7/7 VTA ROIs).

Additionally, it was observed that a subset of axon ROIs would greatly increase fluorescence at seemingly random timepoints and remain elevated for the rest of the trial. This activity could be due to the axons being unhealthy and filling with calcium. Therefore, we identified these axons using the *cusum* function in matlab to detect changes in mean activity that remained elevated for at least 2000 frames or at least 500 frames if they were still elevated at the end of the recording session and removed them from analysis(20/110 LC ROIs, 0/7 VTA ROIs).

4.8. Behavioral Analysis

Mouse velocity was calculated as the change in VR position divided by the sampling rate and smoothed using a Savitzky-Golay filter with a 7 frame window and 5 degree polynomial. To find the lap mean velocity, periods where the mice were immobile (velocity ¡ 5 cm/s) were removed and the average velocity during the remaining frames was calculated. The lap mean freezing ratio was calculated as the number of frames spent immobile (velocity ¡ 0.2 cm/s) divided by the total number of frames for each lap.

4.9. Axon Imaging Analysis

For the three measures below, to avoid weighting axons with a high SNR more than others each ROI was normalized by $(\Delta F/F - \Delta F/Fmin)/(\Delta F/Fmax - \Delta F/Fmin)$ where $\Delta F/Fmin$ is the 1st quantile and $\Delta F/Fmax$ was the 99 quantile for each ROI. The 1st and 99th quantiles were used in order to avoid normalize to noisy outlier data points.

4.10. Position binned fluorescence

To find the position binned fluorescent activity of each ROI, the track was divided into 5 cm bins. For each lap, the average fluorescence in each bin was calculated for each ROI. The position binned fluorescence was then averaged across all laps in each environment to find the mean position binned activity in the familiar and novel environments.

4.11. Velocity binned fluorescent activity

To find the velocity binned fluorescent activity for each ROI, the velocity was divided into 1 cm/s bins from 1 to 30 cm/s. Velocities above this 14 cm/s were excluded from figures because not all mice ran faster than 14 cm/s. For each lap, the ROIs average fluorescence in each velocity bin was calculated and then averaged across all laps in each environment to find the velocity binned activity in the familiar and novel environments.

4.12. Motion initiation aligned fluorescence

Periods where mice were immobile (velocity ¡ 5 cm/s) for at least 1.5s then proceed to run (velocity $\geq$ 5cm/s) for at least 3s were identified. The fluorescent activity for ROIs for these periods was aligned to the frame mice began running (velocity crossed above 5cm/s). The average aligned fluorescent activity of each ROI was then determined for each environment.

4.13. Linear regression analysis

To assess dynamics between each of the above measures and calcium activity of LC and VTA axons, we performed linear regression on the population's familiar environment data and significance was assessed with an F test. To compare the dynamics between LC and VTA axons, we performed exact testing based on Monte-Carlo resampling (1000 resamples with sample size matching the lower sample size condition) as detailed in legends (Fig 1E).

To assess the changing position and velocity encoding of LC axons following exposure to a novel environment, we performed linear regression on the population fluorescence data of the average of the last 4 laps in the familiar environment, and each of the first three laps in the novel environment for each measure. The significance for the fit of each line was assessed with an F test, and an ANCOVA was conducted to test for differences in slope between the four laps. The same process was conducted for the motion initiation dynamics, but only using ROIs in mice who paused within the first 2 laps and 30s following exposure to the novel environment.

4.14. Novel response analysis

To examine the response of LC and VTA axons to the novel VR environment, the fluorescence data was normalized by the mean for each ROIs and aligned to the frame where the mice were switched to the novel environment and the mean normalized F for LC and VTA ROIs at each time point was calculated. Baseline fluorescent activity was then calculated for LC and VTA ROIs separately by generating 1000 shuffled traces of the ROIs calcium activity and subsampling down to the sample size (90 for LC; 7 for VTA) 1000 times and finding the mean of the subsampled shuffles. The mean and 95% CI of all 1000 subsamples was found and the mean activity of LC and VTA ROIs was considered significantly elevated when it passed above the 95% CI of the shuffled data. The same process was repeated to define a baseline for the time binned data (fluorescent activity divided into 50 frame bins) and the lap binned data (mean activity for each lap).

Additionally, to account for changes in behavior between the familiar and novel environments, periods where the animals were immobile (velocity $\leq$ 0.2 cm/s) were removed and running periods were concatenated together and aligned to the switch to the novel environment. Here, we again defined a baseline for the time mean traces, time binned activity, and the lap binned activity using the above bootstrapping approach.

4.15. Figure graphics

All figure graphics including Fig 1A-B were created using BioRender.com.

4.16. Code availability

Scripts used for data analysis are available on Github (x)

4.17. Acknowledgements

We thank Seetha Krishnan and Douglas Goodsmith for feedback on the manuscript. This work was supported by The Whitehall Foundation, The Searle Scholars Program, The Sloan Foundation, The University of Chicago Institute for Neuroscience start-up funds, the NIH 1DP2NS111657-01, and the NIH BRAIN Initiative RF1NS127123 awarded to M.S. and a T32 training grant T32DA043469 from National Institute on Drug Abuse awarded to C.H.

4.18. Author contributions

C.H. and M.S. conceived and designed the experiments. C.H. collected and analyzed the data. C.H. and M.S. interpreted the data and wrote the manuscript.

4.19. Declaration of interests

The authors declare no competing interests.

References

[1] Weber C.N. da Silva, Cristiano C. Köhler, Andressa Radiske, and Martín Cammarota. D1/D5 dopamine receptors modulate spatial memory formation. *Neurobiology of Learning and Memory*, 97(2):271–275, February 2012. ISSN 1074-7427. doi: 10.1016/j.nlm.2012.01.005. URL `https://www.sciencedirect.com/science/article/pii/S1074742712000068`.

[2] Aude Retailleau and Genela Morris. Spatial Rule Learning and Corresponding CA1 Place Cell Reorientation Depend on Local Dopamine Release. *Current Biology*, 28(6):836–846.e4, March 2018. ISSN 09609822. doi: 10.1016/j.cub.2018.01.081. URL `https://linkinghub.elsevier.com/retrieve/pii/S0960982218301477`.

[3] Theodoros Tsetsenis, Julia Kathleen Badyna, Manivanan Subramaniyan, Rebecca Li, Kechun Yang, and John A. Dani. Dopamine and Norepinephrine Modulate the Formation of Aversive Memories in the Hippocampus. *SSRN Electronic Journal*, 2019. ISSN 1556-5068. doi: 10.2139/ssrn.3509875. URL `https://www.ssrn.com/abstract=3509875`.

[4] N. Hansen and D. Manahan-Vaughan. Dopamine D1/D5 Receptors Mediate Informational Saliency that Promotes Persistent Hippocampal Long-Term Plasticity. *Cerebral Cortex*, 24 (4):845–858, April 2014. ISSN 1047-3211, 1460-2199. doi: 10.1093/cercor/bhs362. URL https://academic.oup.com/cercor/article-lookup/doi/10.1093/cercor/bhs362.

[5] Marie E. Gibbs and Roger J. Summers. Role of adrenoceptor subtypes in memory consolidation. *Progress in Neurobiology*, 67(5):345–391, August 2002. ISSN 0301-0082. doi: 10.1016/s0301-0082(02)00023-0.

[6] Steven A. Thomas. Neuromodulatory Signaling in Hippocampus-Dependent Memory Retrieval. *Hippocampus*, 25(4):415–431, April 2015. ISSN 1050-9631. doi: 10.1002/hipo.22394. URL https://www.ncbi.nlm.nih.gov/pmc/articles/PMC9484472/.

[7] Marion Agnès Emma André, Oliver T. Wolf, and Denise Manahan-Vaughan. Beta-adrenergic receptors support attention to extinction learning that occurs in the absence, but not the presence, of a context change. *Frontiers in Behavioral Neuroscience*, 9:125, 2015. ISSN 1662-5153. doi: 10.3389/fnbeh.2015.00125.

[8] Hardy Hagena and Denise Manahan-Vaughan. Differentiation in the protein synthesis-dependency of persistent synaptic plasticity in mossy fiber and associational/commissural CA3 synapses in vivo. *Frontiers in Integrative Neuroscience*, 7, 2013. ISSN 1662-5145. doi: 10.3389/fnint.2013.00010. URL http://journal.frontiersin.org/article/10.3389/fnint.2013.00010/abstract.

[9] Hong-Yuan Chu, Qianqian Wu, Shanglin Zhou, Xiaohua Cao, Ao Zhang, Guo-Zhang Jin, Guo-Yuan Hu, and Xuechu Zhen. SKF83959 suppresses excitatory synaptic transmission in rat hippocampus via a dopamine receptor-independent mechanism. *Journal of Neuroscience Research*, 89(8):1259–1266, August 2011. ISSN 03604012. doi: 10.1002/jnr.22653. URL http://doi.wiley.com/10.1002/jnr.22653.

[10] Hilary T. Edison and Carolyn W. Harley. Medial and lateral perforant path evoked potentials are selectively modulated by pairing with glutamatergic activation of locus coeruleus in the dentate gyrus of the anesthetized rat. *Hippocampus*, 22(3):501–509, March 2012. ISSN 1098-1063. doi: 10.1002/hipo.20916.

[11] Hardy Hagena and Denise Manahan-Vaughan. Learning-facilitated long-term depression and long-term potentiation at mossy fiber-CA3 synapses requires activation of -adrenergic receptors. *Frontiers in Integrative Neuroscience*, 6:23, 2012. ISSN 1662-5145. doi: 10.3389/fnint.2012.00023.

[12] Jinzhong Jeremy Goh and Denise Manahan-Vaughan. Hippocampal long-term depression in freely behaving mice requires the activation of beta-adrenergic receptors. *Hippocampus*, 23(12):1299–1308, December 2013. ISSN 1098-1063. doi: 10.1002/hipo.22168.

[13] Elke Edelmann and Volkmar Lessmann. Dopaminergic innervation and modulation of hippocampal networks. *Cell and Tissue Research*, 373(3):711–727, September 2018. ISSN 1432-0878. doi: 10.1007/s00441-018-2800-7. URL https://doi.org/10.1007/s00441-018-2800-7.

[14] M. Segal, H. Markram, and G. Richter-Levin. Actions of norepinephrine in the rat hippocampus. *Progress in Brain Research*, 88:323–330, 1991. ISSN 0079-6123. doi: 10.1016/s0079-6123(08)63819-4.

[15] Clifford G Kentros, Naveen T Agnihotri, Samantha Streater, Robert D Hawkins, and Eric R Kandel. Increased Attention to Spatial Context Increases Both Place Field Stability and Spatial Memory. *Neuron*, 42(2):283–295, April 2004. ISSN 0896-6273. doi: 10.1016/S0896-6273(04)00192-8. URL https://doi.org/10.1016/S0896-6273(04)00192-8. Publisher: Elsevier.

[16] J. O'Keefe and J. Dostrovsky. The hippocampus as a spatial map. Preliminary evidence from unit activity in the freely-moving rat. *Brain Research*, 34(1):171–175, November 1971. ISSN 00068993. doi: 10.1016/0006-8993(71)90358-1. URL https://linkinghub.elsevier.com/retrieve/pii/0006899371903581.

[17] Tomonori Takeuchi, Adrian J. Duszkiewicz, Alex Sonneborn, Patrick A. Spooner, Miwako Yamasaki, Masahiko Watanabe, Caroline C. Smith, Guillén Fernández, Karl Deisseroth, Robert W. Greene, and Richard G. M. Morris. Locus coeruleus and dopaminergic consolidation of everyday memory. *Nature*, 537(7620):357–362, September 2016. ISSN 0028-0836, 1476-4687. doi: 10.1038/nature19325. URL http://www.nature.com/articles/nature19325.

[18] Philip A. Adeniyi, Amita Shrestha, and Olalekan M. Ogundele. Distribution of VTA Glutamate and Dopamine Terminals, and their Significance in CA1 Neural Network Activity. *Neuroscience*, 446:171–198, October 2020. ISSN 1873-7544. doi: 10.1016/j.neuroscience.2020.06.045.

[19] Tolulope Adeyelu and Olalekan M. Ogundele. VTA multifaceted modulation of CA1 local circuits. *Neurobiology of Learning and Memory*, 202:107760, July 2023. ISSN 10747427. doi: 10.1016/j.nlm.2023.107760. URL https://linkinghub.elsevier.com/retrieve/pii/S1074742723000412.

[20] Zev B Rosen, Stephanie Cheung, and Steven A Siegelbaum. Midbrain dopamine neurons bidirectionally regulate CA3-CA1 synaptic drive. *Nature Neuroscience*, 18(12):1763–1771, December 2015. ISSN 1097-6256, 1546-1726. doi: 10.1038/nn.4152. URL http://www.nature.com/articles/nn.4152.

[21] Colin G McNamara, Álvaro Tejero-Cantero, Stéphanie Trouche, Natalia Campo-Urriza, and David Dupret. Dopaminergic neurons promote hippocampal reactivation and spatial memory persistence. *Nature Neuroscience*, 17(12):1658–1660, December 2014. ISSN 1546-1726. doi: 10.1038/nn.3843. URL https://doi.org/10.1038/nn.3843.

[22] Omar Mamad, Lars Stumpp, Harold M. McNamara, Charu Ramakrishnan, Karl Deisseroth, Richard B. Reilly, and Marian Tsanov. Place field assembly distribution encodes preferred locations. *PLOS Biology*, 15(9):e2002365, September 2017. doi: 10.1371/journal.pbio.2002365. URL https://doi.org/10.1371/journal.pbio.2002365. Publisher: Public Library of Science.

[23] Seetha Krishnan, Chad Heer, Chery Cherian, and Mark E. J. Sheffield. Reward expectation extinction restructures and degrades CA1 spatial maps through loss of a dopaminergic reward proximity signal. *Nature Communications*, 13 (1):6662, November 2022. ISSN 2041-1723. doi: 10.1038/s41467-022-34465-5. URL https://www.nature.com/articles/s41467-022-34465-5.

[24] Kimberly A. Kempadoo, Eugene V. Mosharov, Se Joon Choi, David Sulzer, and Eric R. Kandel. Dopamine release from the locus coeruleus to the dorsal hippocampus promotes spatial learning and memory. *Proceedings of the National Academy of Sciences*, 113(51):14835–14840, December 2016. doi: 10.1073/pnas.1616515114. URL https://www.pnas.org/doi/10.1073/pnas.1616515114. Publisher: Proceedings of the National Academy of Sciences.

[25] Akiko Wagatsuma, Teruhiro Okuyama, Chen Sun, Lillian M. Smith, Kuniya Abe, and Susumu Tonegawa. Locus coeruleus input to hippocampal CA3 drives single-trial learning of a novel context. *Proceedings of the National Academy of Sciences*, 115 (2):E310–E316, January 2018. ISSN 0027-8424, 1091-6490. doi: 10.1073/pnas.1714082115. URL http://www.pnas.org/lookup/doi/10.1073/pnas.1714082115.

[26] Alexandra Mansell Kaufman, Tristan Geiller, and Attila Losonczy. A Role for the Locus Coeruleus in Hippocampal CA1 Place Cell Reorganization during Spatial Reward Learning. *Neuron*, 105(6):1018–1026.e4, March 2020. ISSN 0896-6273. doi: 10.1016/j.neuron.2019.12.029. URL https://www.sciencedirect.com/science/article/pii/S0896627319310955.

[27] Adrian J. Duszkiewicz, Colin G. McNamara, Tomonori Takeuchi, and Lisa Genzel. Novelty and Dopaminergic Modulation of Memory Persistence: A Tale of Two Systems. *Trends in Neurosciences*, 42(2):102–114, February 2019. ISSN 0166-2236. doi: 10.1016/j.tins.2018.10.002. URL https://www.sciencedirect.com/science/article/pii/S016622361830273X.

[28] Ben Engelhard, Joel Finkelstein, Julia Cox, Weston Fleming, Hee Jae Jang, Sharon Ornelas, Sue Ann Koay, Stephan Y. Thiberge, Nathaniel D. Daw, David W. Tank, and Ilana B. Witten. Specialized coding of sensory, motor and cognitive variables in VTA dopamine neurons. *Nature*, 570(7762):509–513, June 2019. ISSN 1476-4687. doi: 10.1038/s41586-019-1261-9. URL https://doi.org/10.1038/s41586-019-1261-9.

[29] Akira Uematsu, Bao Zhen Tan, Edgar A. Ycu, Jessica Sulkes Cuevas, Jenny Koivumaa, Felix Junyent, Eric J. Kremer, Ilana B. Witten, Karl Deisseroth, and Joshua P. Johansen. Modular organization of the brainstem noradrenaline system coordinates opposing learning states. *Nature Neuroscience*, 20(11):1602–1611, November 2017. ISSN 1546-1726. doi: 10.1038/nn.4642.

[30] Shahryar Noei, Ioannis S. Zouridis, Nikos K. Logothetis, Stefano Panzeri, and Nelson K. Totah. Distinct ensembles in the noradrenergic locus coeruleus are associated with diverse cortical states. *Proceedings of the National Academy of Sciences*, 119(18):e2116507119, May 2022. doi: 10.1073/pnas.2116507119. URL https://www.pnas.org/doi/10.1073/pnas.2116507119. Publisher: Proceedings of the National Academy of Sciences.

[31] Daniel J. Chandler, Wen-Jun Gao, and Barry D. Waterhouse. Heterogeneous organization of the locus coeruleus projections to prefrontal and motor cortices. *Proceedings of the National Academy of Sciences of the United States of America*, 111(18):6816–6821, May 2014. ISSN 1091-6490. doi: 10.1073/pnas.1320827111.

[32] Xiaoxi Zhuang, Justine Masson, Jay A. Gingrich, Stephen Rayport, and René Hen. Targeted gene expression in dopamine and serotonin neurons of the mouse brain. *Journal of Neuroscience Methods*, 143(1):27–32, April 2005. ISSN 01650270. doi: 10.1016/j.jneumeth.2004.09.020. URL https://linkinghub.elsevier.com/retrieve/pii/S0165027004003504.

[33] Jacob Reimer, Matthew J McGinley, Yang Liu, Charles Rodenkirch, Qi Wang, David A McCormick, and Andreas S Tolias. Pupil fluctuations track rapid changes in adrenergic and cholinergic activity in cortex. *Nature Communications*, 7(1), December 2016. ISSN 2041-1723. doi: 10.1038/ncomms13289. URL http://www.nature.com/articles/ncomms13289.

[34] John E. Lisman and Anthony A. Grace. The Hippocampal-VTA Loop: Controlling the Entry of Information into Long-Term Memory. *Neuron*, 46(5):703–713, June 2005. ISSN 0896-6273. doi: 10.1016/j.neuron.2005.05.002. URL https://www.sciencedirect.com/science/article/pii/S0896627305003971.

[35] Mark W. Howe, Patrick L. Tierney, Stefan G. Sandberg, Paul E. M. Phillips, and Ann M. Graybiel. Prolonged dopamine signalling in striatum signals proximity and value of distant rewards. *Nature*, 500(7464):575–579, August 2013. ISSN 1476-4687. doi: 10.1038/nature12475. URL https://doi.org/10.1038/nature12475.

[36] HyungGoo R. Kim, Athar N. Malik, John G. Mikhael, Pol Bech, Iku Tsutsui-Kimura, Fangmiao Sun, Yajun Zhang, Yulong Li, Mitsuko Watabe-Uchida, Samuel J. Gershman, and Naoshige Uchida. A Unified Framework for Dopamine Signals across Timescales. *Cell*, 183(6):1600–1616.e25, December 2020. ISSN 0092-8674. doi: 10.1016/j.cell.2020.11.013. URL https://www.sciencedirect.com/science/article/pii/S0092867420315300.

[37] Tanisha D. London, Julia A. Licholai, Ilona Szczot, Mohamed A. Ali, Kimberly H. LeBlanc, Wambura C. Fobbs, and Alexxai V. Kravitz. Coordinated Ramping of Dorsal Striatal Pathways preceding Food Approach and Consumption. *The Journal of Neuroscience*, 38(14):3547–3558, April 2018. ISSN 0270-6474, 1529-2401. doi: 10.1523/JNEUROSCI.2693-17.2018. URL http://www.jneurosci.org/lookup/doi/10.1523/JNEUROSCI.2693-17.2018.

[38] Huijeong Jeong, Annie Taylor, Joseph R Floeder, Martin Lohmann, Stefan Mihalas, Brenda Wu, Mingkang Zhou, Dennis A Burke, and Vijay Mohan K Namboodiri. Mesolimbic dopamine release conveys causal associations. *Science*, 378(6626):eabq6740, December 2022. ISSN 0036-8075, 1095-9203. doi: 10.1126/science.abq6740. URL https://www.science.org/doi/10.1126/science.abq6740.

[39] Elke Edelmann and Volkmar Lessmann. Dopamine Modulates Spike Timing Dependent Plasticity and Action Potential Properties in CA1 Pyramidal Neurons of Acute Rat Hippocampal Slices. *Frontiers in Synaptic Neuroscience*, 3, 2011. ISSN 1663-3563. URL https://www.frontiersin.org/articles/10.3389/fnsyn.2011.00006.

[40] Mark E.J. Sheffield, Michael D. Adoff, and Daniel A. Dombeck. Increased Prevalence of Calcium Transients across the Dendritic Arbor during Place Field Formation. *Neuron*, 96(2):490–504.e5, October 2017. ISSN 0896-6273. doi: 10.1016/j.neuron.2017.09.029. URL https://www.sciencedirect.com/science/article/pii/S0896627317308735.

[41] Can Dong, Antoine D. Madar, and Mark E. J. Sheffield. Distinct place cell dynamics in CA1 and CA3 encode experience in new environments. *Nature Communications*, 12(1):2977, May 2021. ISSN 2041-1723. doi: 10.1038/s41467-021-23260-3. URL https://doi.org/10.1038/s41467-021-23260-3.

[42] Jeffrey L. Gauthier and David W. Tank. A Dedicated Population for Reward Coding in the Hippocampus. *Neuron*, 99(1):179–193.e7, July 2018. ISSN 0896-6273. doi: 10.1016/j.neuron.2018.06.008. URL https://www.sciencedirect.com/science/article/pii/S0896627318304768.

[43] Romain Bourboulou, Geoffrey Marti, François-Xavier Michon, Elissa El Feghaly, Morgane Nouguier, David Robbe, Julie Koenig, and Jerome Epsztein. Dynamic control of hippocampal spatial coding resolution by local visual cues. *eLife*, 8:e44487, March 2019. ISSN 2050-084X. doi: 10.7554/eLife.44487. URL https://doi.org/10.7554/eLife.44487. Publisher: eLife Sciences Publications, Ltd.

[44] Ji-Chuan Zhang, Pak-Ming Lau, and Guo-Qiang Bi. Gain in sensitivity and loss in temporal contrast of STDP by dopaminergic modulation at hippocampal synapses. *Proceedings of the National Academy of Sciences*, 106(31):13028–13033, August 2009. doi: 10.1073/pnas.0900546106. URL https://www.pnas.org/doi/full/10.1073/pnas.0900546106. Publisher: Proceedings of the National Academy of Sciences.

[45] Roger L. Redondo and Richard G. M. Morris. Making memories last: the synaptic tagging and capture hypothesis. *Nature Reviews. Neuroscience*, 12(1):17–30, January 2011. ISSN 1471-0048. doi: 10.1038/nrn2963.

[46] Miwako Yamasaki and Tomonori Takeuchi. Locus Coeruleus and Dopamine-Dependent Memory Consolidation. *Neural Plasticity*, 2017:1–15, 2017. ISSN 2090-5904, 1687-5443. doi: 10.1155/2017/8602690. URL https://www.hindawi.com/journals/np/2017/8602690/.

[47] J.A Ihalainen, P Riekkinen Jr, and M.G.P Feenstra. Comparison of dopamine and noradrenaline release in mouse prefrontal cortex, striatum and hippocampus using microdialysis. *Neuroscience Letters*, 277(2):71–74, December 1999. ISSN 0304-3940. doi: 10.1016/S0304-3940(99)00840-X. URL https://www.sciencedirect.com/science/article/pii/S030439409900840X.

[48] Shaomin Li, William K. Cullen, Roger Anwyl, and Michael J. Rowan. Dopamine-dependent facilitation of LTP induction in hippocampal CA1 by exposure to spatial novelty. *Nature Neuroscience*, 6(5):526–531, May 2003. ISSN 1097-6256, 1546-1726. doi: 10.1038/nn1049. URL http://www.nature.com/articles/nn1049.

[49] David Dupret, Joseph O'Neill, Barty Pleydell-Bouverie, and Jozsef Csicsvari. The reorganization and reactivation of hippocampal maps predict spatial memory performance. *Nature Neuroscience*, 13(8):995–1002, August 2010. ISSN 1097-6256, 1546-1726. doi: 10.1038/nn.2599. URL http://www.nature.com/articles/nn.2599.

[50] Jeremy D Cohen, Mark Bolstad, and Albert K Lee. Experience-dependent shaping of hippocampal CA1 intracellular activity in novel and familiar environments. *eLife*, 6, July 2017. ISSN 2050-

084X. doi: 10.7554/eLife.23040. URL https://elifesciences.org/articles/23040.

[51] Ananya Chowdhury, Alessandro Luchetti, Giselle Fernandes, Daniel Almeida Filho, George Kastellakis, Alexandra Tzilivaki, Erica M. Ramirez, Mary Y. Tran, Panayiota Poirazi, and Alcino J. Silva. A locus coeruleus-dorsal CA1 dopaminergic circuit modulates memory linking. *Neuron*, page S0896627322007073, August 2022. ISSN 08966273. doi: 10.1016/j.neuron.2022.08.001. URL https://linkinghub.elsevier.com/retrieve/pii/S0896627322007073.

[52] Karine Ramires Lima, Liane da Silva de Vargas, Bruna Ramborger, Rafael Roehrs, Dieuwke Sevenster, Iván Izquierdo, Rudi D'Hooge, and Pâmela B Mello-Carpes. Noradrenergic and dopaminergic involvement in novelty modulation of aversive memory generalization of adult rats. *Behavioural Brain Research*, 371:111991, October 2019. ISSN 0166-4328. doi: 10.1016/j.bbr.2019.111991. URL https://www.sciencedirect.com/science/article/pii/S0166432819303201.

[53] Perla Moreno-Castilla, Rodrigo Pérez-Ortega, Valeria Violante-Soria, Israela Balderas, and Federico Bermúdez-Rattoni. Hippocampal release of dopamine and norepinephrine encodes novel contextual information. *Hippocampus*, 27(5):547–557, May 2017. ISSN 1050-9631. doi: 10.1002/hipo.22711. URL https://doi.org/10.1002/hipo.22711. Publisher: John Wiley & Sons, Ltd.

[54] D.L. Cimarusti, K. Saito, J.E. Vaughn, R. Barber, E. Roberts, and P.E. Thomas. Immunocytochemical localization of dopamine--hydroxylase in rat locus coeruleus and hypothalamus. *Brain Research*, 162(1):55–67, February 1979. ISSN 0006-8993. doi: 10.1016/0006-8993(79)90755-8. URL https://www.sciencedirect.com/science/article/pii/0006899379907558.

[55] G. L. Shulman, R. W. Remington, and J. P. McLean. Moving attention through visual space. *Journal of Experimental Psychology. Human Perception and Performance*, 5(3):522–526, August 1979. ISSN 0096-1523. doi: 10.1037//0096-1523.5.3.522.

[56] Sebastien Bouret and Susan J. Sara. Locus coeruleus activation modulates firing rate and temporal organization of odour-induced single-cell responses in rat piriform cortex. *The European Journal of Neuroscience*, 16(12):2371–2382, December 2002. ISSN 0953-816X. doi: 10.1046/j.1460-9568.2002.02413.x.

[57] Ana Raquel O. Martins and Robert C. Froemke. Coordinated forms of noradrenergic plasticity in the locus coeruleus and primary auditory cortex. *Nature Neuroscience*, 18(10):1483–1492, October 2015. ISSN 1546-1726. doi: 10.1038/nn.4090.

[58] Barry D. Waterhouse and Rachel L. Navarra. The locus coeruleus norepinephrine system and sensory signal processing: A historical review and current perspectives. *Behavioral Consequences of Noradrenergic Actions in Sensory Networks*, 1709:1–15, April 2019. ISSN 0006-8993. doi: 10.1016/j.brainres.2018.08.032. URL https://www.sciencedirect.com/science/article/pii/S0006899318304542.

[59] Noah L. Pettit, Xintong C. Yuan, and Christopher D. Harvey. Hippocampal place codes are gated by behavioral engagement. *Nature Neuroscience*, 25(5):561–566, May 2022. ISSN 1546-1726. doi: 10.1038/s41593-022-01050-4. URL https://doi.org/10.1038/s41593-022-01050-4.

[60] Daniel A. Dombeck, Christopher D. Harvey, Lin Tian, Loren L. Looger, and David W. Tank. Functional imaging of hippocampal place cells at cellular resolution during virtual navigation. *Nature Neuroscience*, 13(11):1433–1440, November 2010. ISSN 1546-1726. doi: 10.1038/nn.2648. URL https://www.nature.com/articles/nn.2648. Number: 11 Publisher: Nature Publishing Group.

[61] James G. Heys, Krsna V. Rangarajan, and Daniel A. Dombeck. The functional micro-organization of grid cells revealed by cellular-resolution imaging. *Neuron*, 84(5):1079–1090, December 2014. ISSN 1097-4199. doi: 10.1016/j.neuron.2014.10.048.

[62] Dmitriy Aronov and David W. Tank. Engagement of neural circuits underlying 2D spatial navigation in a rodent virtual reality system. *Neuron*, 84(2):442–456, October 2014. ISSN 1097-4199. doi: 10.1016/j.neuron.2014.08.042.

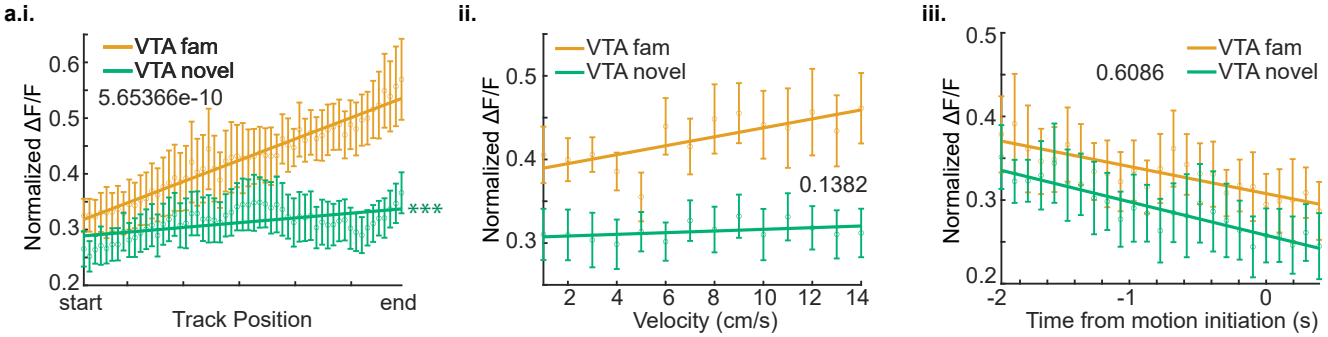

Supplementary Figure 1: **a,i,** Population average position binned $\Delta F/F \pm$ s.e.m. of VTA ROIs (n = 7 ROIs in 7 mice) in the familiar (orange) and novel (green) rewarded environments. Linear regression, F test, Rewarded, $P < 1e-21$, Unrewarded, $P < 0.01$. **ii,** Same data as (a,i) binned by velocity. Linear regression, F test, Rewarded, $P < 0.05$, Unrewarded, $P = 0.57$. **iii,** Same data as (a,i) aligned to motion onset. Linear regression, F test, Rewarded, $P < 0.01$, Unrewarded, $P < 0.001$. The slope of each novel measure was compared to the familiar laps using a one-way ANCOVA with Tukey HSD post hoc test. * $P < 0.05$, ** $P < 0.001$, *** $P < 1e-4$.